Spatial Separation of Closely-Spaced Users in Measured Massive Multi-User MIMO Channels

Flordelis, Jose; Gao, Xiang; Dahman, Ghassan; Rusek, Fredrik; Edfors, Ove; Tufvesson, Fredrik

Published in:
2015 IEEE International Conference on Communications (ICC)

2015

Spatial Separation of Closely-Spaced Users in Measured Massive Multi-User MIMO Channels

Jose Flordelis, Xiang Gao, Ghassan Dahman, Fredrik Rusek, Ove Edfors and Fredrik Tufvesson

Dept. of Electrical and Information Technology, Lund University, Lund, Sweden
Email: *firstname.lastname*@eit.lth.se

***Abstract*—Fully-synchronous measurements of a massive multi-user multiple-input multiple-output (MU-MIMO) radio propagation channel are presented. We evaluate the ability of a massive MIMO system to spatially separate users located close to each other in line-of-sight (LOS) propagation conditions. The system consists of a base-station (BS) antenna array equipped with 64 dual-polarized antenna elements (128 ports) arranged in a cylindrical configuration, and eight single-antenna users. The users are confined to a five-meter diameter circle and move randomly at pedestrian speeds. The BS antenna array is located on top of a 20 m tall building and has LOS to the users. We examine user separability by studying singular value spread of the MU-MIMO channel matrix for several subsets of BS antenna array ports, along with sum-rate capacity and achievable sum-rates with both zero-forcing and matched-filtering linear precoders. We also analyze the performance of the user with the lowest rate. Finally, a comparison between the performance offered by the massive MIMO system and that of a conventional MU-MIMO system is provided. To the best of our knowledge, this is the first report of fully-synchronous dynamic measurements of a massive MIMO system. Our investigation shows that even users located close to each other in LOS propagation conditions can be spatially separated in a massive MIMO system.**

***Keywords*—multi-user multiple-input multiple-output systems, MU-MIMO, massive MIMO, large-scale MIMO, MIMO channel measurements, spatial separation, singular value spread, sum-rate capacity, sum-rate, linear precoder.**

I. Introduction

Massive MIMO is an emerging communication technology promising order-of-magnitude improvements in data throughput, link reliability, range, and transmit-energy efficiency [1]–[4]. These benefits arise from leveraging additional degrees of freedom provided by an excess of antenna elements at the BS side. A typical massive MIMO system can consist of one or more BSs equipped with many, say, $M = 100$, antenna elements serving K single-antenna users in the same time-frequency resource. K is in the order of 10 to 20 users, possibly more. Due to its potential to greatly increase spectral efficiency compared to today's systems, massive MIMO is considered as one of the main directions towards future 5G communication systems [5]–[7].

A key assumption when addressing massive MIMO systems is so-called *favorable* propagation conditions, meaning that propagation channels to different users are nearly orthogonal. Under this assumption, the scaled Gram matrix $\mathbf{G} = \mathbf{H}\mathbf{H}^{\mathrm{H}}/M$, where $\mathbf{H}$ is the channel matrix, approaches a diagonal matrix as M goes to infinity. Hence, linear precoding and detection schemes such as zero-forcing (ZF) and matched-filtering (MF) become nearly optimal [1], [2], [8]. Nevertheless, in real propagation channels and with practical setups, the off-diagonal entries of $\mathbf{G}$ typically have non-zero values. User separation based on spatial channel properties is particularly difficult in situations where the users are located close to each other and experience LOS propagation conditions to the BS antenna array.

Several measurement campaigns have been conducted to study the performance of massive MIMO in real propagation environments. In [9]–[11], we reported outdoor massive MIMO channel measurements at 2.6 GHz with a linear array and a cylindrical array, both having 128 antenna elements. The investigations concluded that real propagation channels allow effective use of massive MIMO technology in the sense that a large fraction of the sum-rate capacity of MIMO channels with independent and identically distributed (i.i.d.) Rayleigh fading can be achieved in real propagation channels: as the number of BS antenna elements increases, the orthogonality among users' channels increases, and linear precoding schemes achieve a performance close to that of dirty-paper coding (DPC) [12]. This is also shown in [8] for indoor BS measurements. In [13] massive MIMO channel measurements using a scalable antenna array consisting of up to 112 elements were reported. The results in [13] further support the conclusions drawn in [8], [10], [11], that theoretical gains of massive MIMO can be achieved in practice. Altogether, the combined set of published experimental results on massive MIMO elevates it from a mere theoretical concept to a practical technology.

Here we present a new massive MIMO channel measurement campaign at 2.6 GHz. Similar to [8] and [11] we use a cylindrical array with 128 ports, although the presented campaign differs from those previously reported in two important ways:

- Instead of having virtual users, i.e., choosing users from different measurement positions, as in [8]–[11], we have fully-synchronous dynamic measurements to multiple users. This means that the channels from all users to the BS antenna array are measured simultaneously, and we can capture joint statistical properties of the multi-user channels and their evolution in time, i.e., the dynamics of the system. To the best of our knowledge, this is the first paper reporting such measurements for a massive MIMO system.
- With the obtained measurement data, we focus on investigating the spatial separation of closely-spaced users in LOS, which is a particularly difficult situation

(a) (b)

Fig. 1. (a) The cylindrical array with 128 ports. (b) View from site MS 2.

(a) (b)

Fig. 2. (a) A user holding the user equipment antenna with an inclination of 45°. (b) Users moving randomly within the five-meter diameter circle.

for conventional MIMO. For massive MIMO, it is expected that with a large-enough number of antenna elements at the BS, spatial multiplexing of closely-spaced users is possible. Our study is relevant to the scenario of outdoor live concerts or sports events, where user density can be relatively high.

II. Measurement Description

A. Measurement Setup

The measurement campaign was performed using a 128-port cylindrical array at the BS side, shown in Fig. 1, with 16 dual-polarized patch antenna elements in each circle and 4 such circles stacked on top of each other. The spacing of adjacent elements is half a wavelength at 2.6 GHz. At the user side, we use eight vertically-polarized omni-directional antennas[1], acting as eight simultaneous users. The eight antennas are connected through optical fibers to the transmit side of the RUSK LUND MIMO channel sounder [14].

Measurements were recorded using a center frequency of 2.6 GHz and 40 MHz bandwith. Each measurement took 17 seconds, and 300 snapshots were recorded during this time.

[1]The antennas, of type SkyCross SMT-2TO6MB-A, are omni-directional in azimuth when measured without users. The radiation pattern including the users is more complex and is dependent on the exact position of antenna and users.

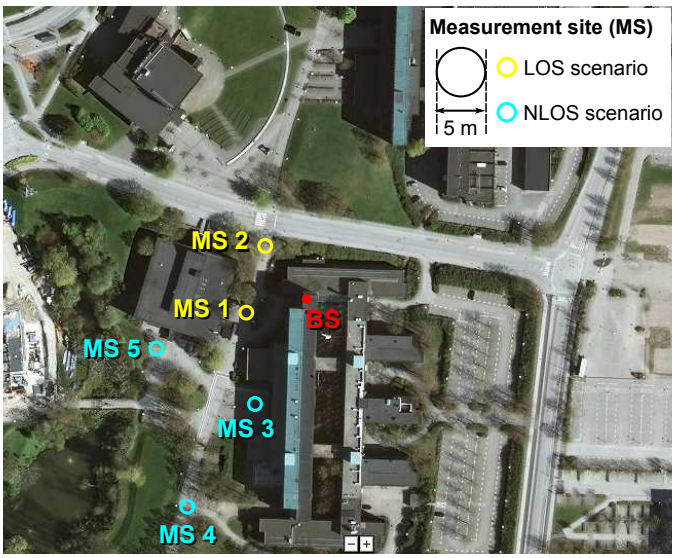

Fig. 3. Overwiew of the measurement area.

The sounding signals were transmitted with 0.5 W output power. Values of the average measurement signal-to-noise ratio (SNR) between 14 dB to 16 dB have been estimated.

B. Measurement Environment

The measurements were carried out outside the main entrace of the E-building of the Faculty of Engineering (LTH), Lund University, Lund, Sweden (55.711510 N, 13.210405 E). The cylindrical array at the BS side was placed on the roof of the E-building, as shown in Fig. 1. At the user side several sites were measured. MS 1 and 2 have LOS conditions to the BS array, while MS 3–5 have NLOS conditions[2] (see Fig. 3). At each site, we have a circle with a five-meter diameter and eight users moving inside it, representing a situation of high user density. During the measurements, the users were holding the antennas inclining them at about 45 degrees, so that we have both vertical and horizontal polarizations at the user side. The eight users were moving randomly at pedestrian speeds around 0.5 m/s, inside the 5 m circle. Note that, since the users were allowed to turn around, the LOS component to the BS can be blocked in some snapshots, by the user holding the antenna or by other users (see Fig. 2).

III. Signal Model

For the analysis, we consider the downlink of a single-cell MU-MIMO system. The system consists of K single-antenna users and a BS equipped with M antenna ports ($K \leq M$). Orthogonal frequency division multiplexing (OFDM) with L subcarriers is assumed. Let $\mathbf{s}_{\ell,n}$ be the $M \times 1$ vector signal transmitted by the BS at subcarrier ℓ and snapshot n, with $1 \leq l \leq L$ and $1 \leq n \leq N$. The composite received signal $\mathbf{y}_{\ell,n}$ can be written as

$$\mathbf{y}_{\ell,n} = \mathbf{H}_{\ell,n}\mathbf{s}_{\ell,n} + \mathbf{w}_{\ell,n}, \quad (1)$$

where $\mathbf{w}_{\ell,n}$ is the $K \times 1$ vector of the receiver noise with independent components distributed as $\mathcal{CN}(0,1)$, and $\mathbf{H}_{\ell,n} \in \mathbb{C}^{K \times M}$ is the narrow-band channel matrix of the radio

[2]In this work we are only concerned with sites in LOS, i.e. MS 1 and MS 2.

propagation channel, satisfying $\mathbb{E}\{\|\mathbf{h}_{k,\ell,n}\|_{\mathrm{F}}^2\} = M$ where $\mathbf{h}_{k,\ell,n}$ is the kth row of $\mathbf{H}_{\ell,n}$. Furthermore, the transmit vector $\mathbf{s}_{\ell,n}$ has a covariance matrix satisfying the power constraint

$$\mathbb{E}\{\mathbf{s}_{\ell,n}^{\mathrm{H}}\mathbf{s}_{\ell,n}\} = P. \tag{2}$$

With these conventions, the mean received power per user in the MISO case with maximum ratio transmission (MRT) becomes $P\frac{M}{K}$, yielding a channel capacity

$$C_{\mathrm{MISO}} = \log_2\left(1 + P\frac{M}{K}\right). \tag{3}$$

In this work, we choose to harvest the array gain as reduced transmit power. Therefore, the total transmit power P is scaled according to

$$P = \rho\frac{K}{M}. \tag{4}$$

In this way, the mean SNR per user in the MISO case with MRT remains constant at some target level ρ.

A. Normalization

In order to compensate for gain imbalances across different MISO links, arising, e.g., from differences in the electronic components used in the measurement setup, channel normalization is applied. The normalization is such that the average energy of the user channels, when taken over all $L = 257$ subcarriers and $N = 300$ measurement snapshots, is equal to 128. This normalization can be obtained by defining

$$\mathbf{h}_{k,\ell,n}^{\mathrm{norm}} = \sqrt{\frac{128LN}{\sum_{n=1}^{N}\sum_{l=1}^{L}\|\mathbf{h}_{k,\ell,n}^{\mathrm{meas}}\|_{\mathrm{F}}^2}}\,\mathbf{h}_{k,\ell,n}^{\mathrm{meas}}, \tag{5}$$

where $\mathbf{h}_{k,\ell,n}^{\mathrm{norm}}$ is the kth normalized MISO channel, i.e., the kth row of the normalized MU-MIMO channel matrix $\mathbf{H}_{\ell,n}^{\mathrm{norm}}$, and $\mathbf{h}_{k,\ell,n}^{\mathrm{meas}}$ represents the *measured* MISO channel from the BS antenna array to the kth user. With the normalization proposed, imbalances in the channel gain of different users are removed, while energy variations over BS antenna elements, subcarriers and measurement times are retained. In particular, the distance-dependent path loss of the radio propagation channel is removed, whereas the effects of small-scale and large-scale fading remain. The sub-indices ℓ and n will be dropped in the rest of the discussion. This will not cause any problem since, from this point on, all processing is done per time-frequency resource.

B. Antenna Array Size Reduction

The effect of the number of antenna elements M at the BS antenna array is a topic of interest for the design and implementation of practical massive MIMO systems. Thus, the 8×128 MU-MIMO channel matrices obtained from the measurements at different sites can be downsampled to a suitable size, $8 \times M$, and the influence of the parameter M can be investigated. Let $8 \le M \le 128$ be the reduced number of antenna elements at the BS antenna array, and $\pi_M = \{p(1), \ldots, p(M)\}$, with $1 \le p(1) < \ldots < p(M) \le M$, a set of indices selecting M antenna elements from a total of 128. Then, the normalized and π_M-reduced channel matrix $\mathbf{H}^{\mathrm{norm},\pi_M}$ is obtained from

$$\mathbf{h}_k^{(\text{col) norm},\pi_M} = \mathbf{h}_{p(k)}^{(\text{col) norm}}, \tag{6}$$

where $\mathbf{h}_k^{(\text{col) norm},\pi_M}$ and $\mathbf{h}_i^{(\text{col) norm}}$ are the kth and ith columns of $\mathbf{H}^{\mathrm{norm},\pi_M}$ and $\mathbf{H}^{\mathrm{norm}}$, respectively.

The antenna elements of the sub-arrays have been selected in the following way: i) for $M = 128$, all antenna patches are used; ii) for $M = 64$, 8 evenly spaced antenna patches are chosen from each antenna ring, with the antenna patches in two adjacent antenna rings staggered by one element; iii) for $M = 32$, the antenna patches of the two middle rings for the case of $M = 64$ are chosen; iv) for $M = 16$, the antenna patches of the lower ring for the case of $M = 32$ are chosen; v) for $M = 8$, the four adjacent antenna patches pointing northwest in the same ring as for the case of $M = 16$ are chosen. In all cases, both ports from each selected antenna patch are used. With this choice, the sub-arrays for the cases of $M = 128, 64, 32$ and 16 are approximately isotropic, while the sub-array for the case of $M = 8$ shows a directional gain of 0.6 dB and 3.8 dB for sites MS 1 and MS 2, respectively. The case $M = 8$ resembles a conventional 8×8 MU-MIMO deployment and, hence, will serve as a baseline for evaluating the performance of massive MIMO.

C. Singular Value Spread

In this section we introduce the singular value spread of the channel matrix $\mathbf{H}$ as a measure of the degree of orthogonality among the users. The channel matrix $\mathbf{H}$ has a singular value decompostion

$$\mathbf{H} = \mathbf{U}\mathbf{\Sigma}\mathbf{V}^{\mathrm{H}}, \tag{7}$$

where $\mathbf{U} \in \mathbb{C}^{K\times K}$ and $\mathbf{V} \in \mathbb{C}^{M\times M}$ are unitary matrices and $\mathbf{\Sigma} \in \mathbb{C}^{K\times M}$ is a diagonal matrix containing the ordered singular values of the channel, $\sigma_1 \ge \ldots \ge \sigma_K \ge 0$. The singular value spread κ (*a.k.a.* condition number) is then defined as the ratio between the largest and the smallest singular values, as given by

$$\kappa = \frac{\sigma_1}{\sigma_K}. \tag{8}$$

It follows that $1 \le \kappa \le \infty$. Values of κ close to 1 indicate nearly full user orthogonality while, under the assumption (5), large values of κ imply a strong linear dependency of, at least, two of the rows in $\mathbf{H}$ and, thereupon, a relative difficulty in the spatial separation of the corresponding users.

D. Dirty-Paper Coding Capacity

The singular value spread is not very informative when it takes large values. For example, consider a radio propagation environment in which the transmit signals from the BS antenna array to two of the users, say user 1 and user 2, reach those users through certain common propagation paths. This situation may lead to almost parallel MISO channels $\mathbf{h}_1$ and $\mathbf{h}_2$ and, as a result, to large singular value spreads. However, the BS antenna array might nonetheless be able to separate the channels of the remaining users. Hence, multiplexing several data streams on the same time-frequency resource is possible even when the singular value spread is large. In this section, the sum-rate capacity of the MU-MIMO downlink channel is introduced as a second measure of the performance of the massive MIMO system.

The sum-rate capacity of the narrow-band MU-MIMO downlink channel with full channel state information (CSI) at the BS is given by [15]

$$C_{\text{DPC}} = \max_{\{\gamma_k\}} \log_2 \det(\mathbf{I}_M + \mathbf{H}^{\text{H}}\mathbf{D}\mathbf{H})$$
$$\text{subject to} \quad \sum_{k=1}^{K} \gamma_k = P, \quad \gamma_k \geq 0, \quad \forall k, \tag{9}$$

with $\mathbf{D} = \text{diag}(\gamma_1, \ldots, \gamma_K)$ and P the total transmit power (2). Problem (9) is a convex problem and can be efficiently solved, for instance, by means of the sum-power iterative waterfilling algorithm described in [16].

E. Linear Precoding

The sum-rate capacity of the narrow-band MU-MIMO downlink channel can be achieved by dirty-paper coding (DPC) [12]. However, the high computational complexity of DPC renders it impractical even for a low number of users. As an alternative to DPC, we consider linear precoding schemes of the form

$$\mathbf{s} = \mathbf{W}\mathbf{x}, \tag{10}$$

where $\mathbf{W} \in \mathbb{C}^{M \times K}$ is the precoding matrix and $\mathbf{x}$ is the $K \times 1$ vector containing the user data streams. We look at the performance of the popular zero-forcing and matched-filtering linear precoders [17]. The ith column of the ZF precoding matrix, $\mathbf{w}_{\text{ZF},i}$, is given by

$$\mathbf{w}_{\text{ZF},i} = \frac{\mathbf{h}_i^{(\dagger)}}{\sqrt{\|\mathbf{h}_i^{(\dagger)}\|_{\text{F}}^2}}, \tag{11}$$

where $\mathbf{h}_i^{(\dagger)}$ is the ith column of $\mathbf{H}^{\text{H}}(\mathbf{H}\mathbf{H}^{\text{H}})^{-1}$, the pseudo-inverse of the channel matrix. The ith column of the MF precoding matrix, $\mathbf{w}_{\text{MF},i}$, is given by

$$\mathbf{w}_{\text{MF},i} = \frac{\mathbf{h}_i^{\text{H}}}{\sqrt{\|\mathbf{h}_i\|_{\text{F}}^2}}. \tag{12}$$

where $\mathbf{h}_i$ is the ith row of $\mathbf{H}$. Optimal allocation of transmit power to the user data streams in $\mathbf{x}$, subject to the sum-power constraint (2), has been performed by means of numerical methods. For the ZF precoder, the product $\mathbf{H}\mathbf{W}_{\text{ZF}}$ is diagonal and optimal power allocation can be achieved by the standard water-filling algorithm [18]. The MF precoding case, however, constitutes a non-convex problem and the numerical methods used in the preparation of this work do not guarantee the optimality of the transmit power allocations obtained.

IV. Performance Evaluation

In this section, we evaluate the ability of massive MIMO at separating users located close to each other in LOS propagation conditions, and compare it with the performance of i.i.d. Rayleigh channels. First, we look at the singular value spread of the measured channels.

The cumulative distribution function (CDF) of the singular value spread in logarithmic units,

$$\kappa_{\text{dB}} = 10 \log_{10} \frac{\sigma_1}{\sigma_K}, \tag{13}$$

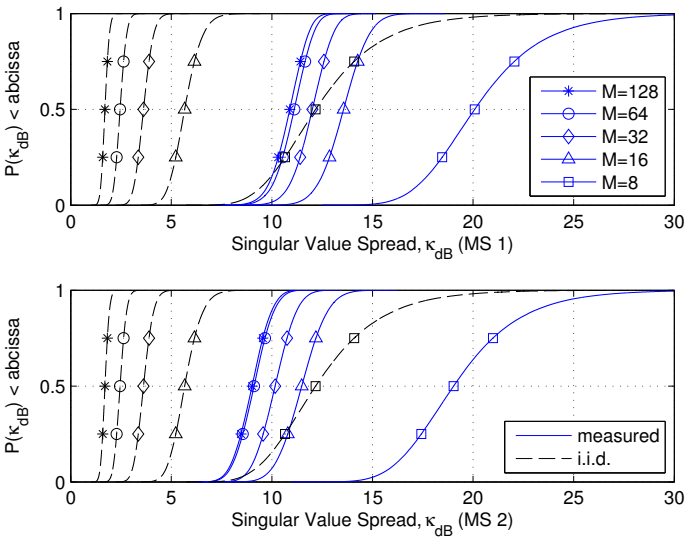

Fig. 4. CDFs of the singular value spread in logarithmic units when using 128, 64, 32, 16 and 8 antenna elements at the BS. In this scenario, eight users are located close to each other within the area of a five-meter diameter circle and experience LOS to the BS antenna array. Plots are given for two different measurement sites, labeled as MS 1 (top) and MS 2 (bottom). For comparison purposes, CDFs of the singular value spread of i.i.d. Rayleigh channels with the same number of antenna elements are also given. Note that the legend is shared between both figures.

when using 128, 64, 32, 16 and 8 antenna elements at the BS, can be seen in Fig. 4. CDFs of the singular value spreads of i.i.d. Rayleigh channels with the same number of transmit and receive antenna elements are also shown.

We can see from Fig. 4 that the measured user channels decorrelate as the number of antenna elements at the BS, M, increases. Furthermore, the slopes of the CDF curves become steeper with increasing values of M, demonstrating the hardening effect of the user channels. The median of the singular value spread for measured channels when using 128 antenna elements at the BS is 10.4 dB and 8.4 dB for sites MS 1 and MS 2, respectively. For both sites, the CDF of the singular value spreads for $M = 64$ is very similar to that of $M = 128$, while a moderate degradation by one to three dB is observed when M is reduced to 32 and 16. By contrast, the median of the singular value spread increases dramatically to 19.6 dB for site MS 1 and to 18.4 dB for site MS 2 when only 8 antenna elements are used at the BS — i.e. a 10 dB loss when comparing conventional MU-MIMO with massive MIMO; a similar increase of the variance is observed.

This information is summarized in Fig. 5, where the CDFs shown in Fig. 4 are represented as points in a coordinate system in which the abcissas correspond to the median of the distribution of the singular value spread, and the ordinates correspond to the inter-quartile range (IQR). In this representation, moving to the left (reduced median) and to the bottom of the figure (reduced IQR) means improved user orthogonality and channel hardening. We see that, for the case of $M = 128$, the median of the channel measured at site MS 1 lies in-between the median of i.i.d. Rayleigh channels with $M = 8$ and $M = 9$, whereas the IQR matches that of an i.i.d. Rayleigh channel with $M = 10$. Hence, one can say that, the measured 8×128 channel has an *effective* degree of orthogonality equivalent to

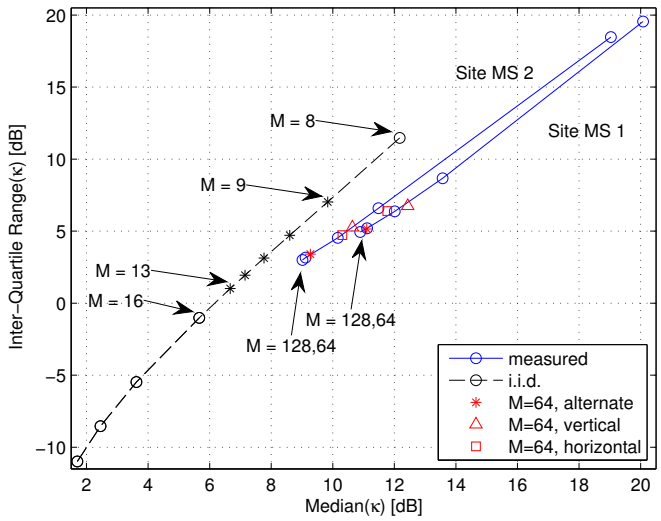

Fig. 5. Median and inter-quartile range (IQR) of the singular value spread for the same cases as in Fig. 4. From left to right, circles represent the cases of $M = 128, 64, 32, 16$ and 8. For i.i.d. Rayleigh channels, dots are used to represent the cases $M = 13, 12, 11, 10$ and 9. Additionally, the medians and the IQRs for the cases of $M = 64$ and vertically-polarized antenna ports only (triangle), horizontally-polarized antenna ports only (square) and antenna ports including both polarizations (star) are also given.

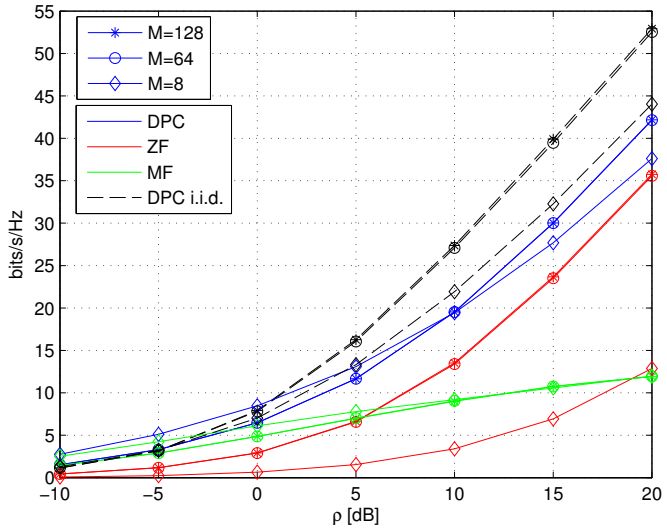

Fig. 6. Ergodic sum-rate capacity at site MS 2 when using 128, 64 and 8 antenna elements at the BS. Transmit power reduction have been applied.

an i.i.d. Rayleigh channel with M between 8 and 9, whereas its *effective* hardening corresponds to $M = 10$. In the same sense, for site MS 2, the behavior of the channel resembles that of an i.i.d. Rayleigh channel with 9–10 BS antenna elements, with a somewhat reduced dispersion ($M = 11$). The large gap between measured channels and synthetic i.i.d. channels can be partly explained by the cylindrical geometry of the BS antenna array: more than half of the antenna array elements cannot "see" the users at sites MS 1 and MS 2.

A further observation that we can make from Fig. 5 is that the improvement in user channel orthogonality when increasing the number of antenna elements at the BS beyond 64 is marginal in comparison with that of i.i.d. Rayleigh channels. This fact might indicate that, for this specific scenario and array geometry, further gains in user spatial separation cannot be obtained by increasing the density of the spatial sampling at the BS. Rather, one must resort to dual-polarized antenna elements, as explained next. On top of the subsets of BS antenna elements thus far discussed, three extra BS antenna array subsets are considered: i) $M = 64$ with all elements vertically polarized, ii) $M = 64$ with all elements horizontally polarized, and iii) $M = 64$ with neighbour elements having alternate polarizations. With this choice, exactly one port from each of the 64 antenna patches of the BS array is selected, for all three subsets. The correponding median and IQR coordinates have been plotted in Fig 5. We see that, to fully extract the diversity offered by the environment, we need to use both vertically and horizontally polarized antenna elements. As a matter of fact (see Fig. 5), when only a single polarization is used the resulting system is roughly equivalent to one with 16 dual-polarized antenna patches ($M = 32$). In other words, if only one polarization mode is used, up to half of the antenna elements have a zero net contribution.

Let us now turn our attention to the sum-rates achievable through massive MIMO in the considered setup by linear precoding. The estimated ergodic sum-rate capacity and ergodic sum-rates for the ZF and MF precoders when using 128, 64 and 8 antenna elements at the BS are shown in Fig. 6 for several target values of ρ. Note that the cases $M = 32$ and $M = 16$ have been dropped since these values of M are not representative of typical massive MIMO deployments. We focus on the sum-rate results for site MS 2 (similar comments apply to site MS 1). Fig. 6 shows that, for moderate values of ρ, massive MIMO with ZF can achieve a large fraction of the DPC capacity. For instance, 69% of the DPC capacity (19.5 bits/s/Hz) is achieved when $\rho = 10$ dB, and this figure increases to 86% (of 42.2 bits/s/Hz) when $\rho = 20$ dB. On the other hand, the sum-rates achievable by the ZF precoder in a conventional 8×8 MU-MIMO setup fall much shorter: 18% and 34% (of 19.4 bits/s/Hz and 37.6 bits/s/Hz, respectively) for the same SNR points. It is important to recall that transmit power has been reduced as described in Sec. III-B: In the case at hand, conventional 8×8 MU-MIMO radiates 38.4 times more power than massive MIMO with $M = 128$. If, rather, the massive MIMO array gain is leveraged to its full extent, an increase of the sum-rate capacity and ZF sum-rate by $K \log_2(\frac{M}{K})$ bits/s/Hz, i.e. 32 bits/s/Hz for $M = 128$, can be expected for moderate values of ρ and beyond.

Finally, we look into the issue of *fairness* in the allocation of the user data rates. As is known, maximizing the sum-rate might result in large imbalances in the data rates allocated to each of the users, with users experiencing advantageous signal strength levels being allocated most of the available sum-rate, and users experiencing weak signal strengths being allocated little or no capacity. The top part of Fig. 7 shows the average number of users allocated power, i.e. the average number of users with $\gamma_k > 0$, at site MS 2 when using 128, 64 and 8 antenna elements at the BS, for DPC, ZF and MF. It can be seen that, with 8×64 massive MIMO and ZF, all 8 users are allocated power for values of $\rho = 10$ dB, or greater. By contrast, at the same SNR point, conventional 8×8 MU-MIMO with ZF allocates power to six users only. Hence, we see that massive MIMO can achieve higher sum-rates and, at the same time, schedule more users than conventional MU-MIMO. On the other hand, conventional MU-MIMO with MF offers a larger sum-rate (see Fig. 6) at the expense of a decrease in

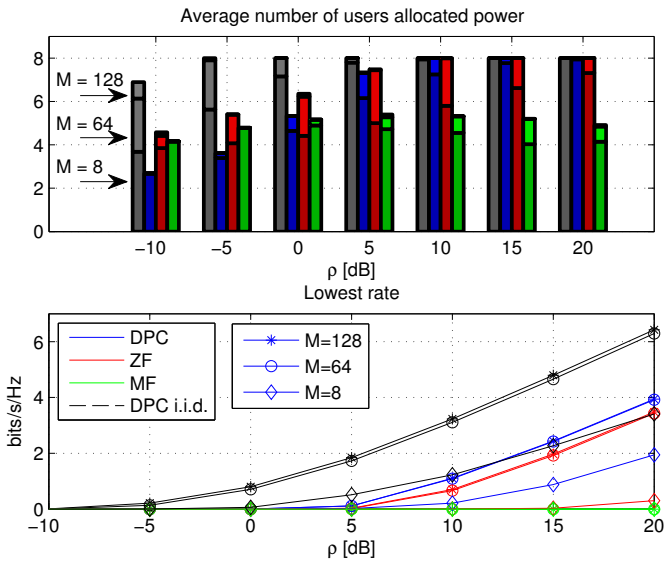

Fig. 7. Average number of users allocated power (top) and lowest ergodic rate (bottom) at site MS 2 when using 128, 64 and 8 antenna elements at the BS. Transmit power reduction has been applied.

user fairness (five or less users scheduled). Additionally, the lowest user rate averaged over all time-frequency resources is shown at the bottom part of Fig. 7. As expected, the lowest user rate for the MF and ZF with conventional 8×8 MU-MIMO is (close to) zero bits/s/Hz.

V. Summary and Conclusions

Let us go back to the question that we tried to answer in this paper: Can massive MIMO spatially separate users that are confined to a circle with a five-meter diameter in LOS conditions? This question is not easy to give a satisfactory answer to, but in an effort to partly address it, we have conducted a measurement campaign which can be summarized as in Table I.

TABLE I. ZF Sum-Rate for Site MS 2 ($\rho = 10\,\mathrm{dB}$).

	M=8	**M=64**
Average number of users allocated power with ZF	6	8
Sum-rate shared among the users	3.4 bit/s/Hz	13.4 bit/s/Hz
Fraction of DPC capacity achieved	18%	69%
Total transmit power shared among the users	3.8 dB	-9.0 dB

In our view, we have demonstrated clear indications that massive MIMO indeed separates them, as, with massive MIMO, many more users can share a much larger sum-rate compared to the case of conventional MIMO. What is more, with massive MIMO, all users get a non-zero communication rate for reasonable SNR values when the sum-rate of the system is maximized. All in all, we think it is fair to say that the massive MIMO system is able to separate all the closely-located users.

VI. Acknowledgements

The authors would like to thank all the participants in this measurement campaign. We would also like to acknowledge the financial support from ELLIIT - an Excellence Center at Linköping-Lund in Information Technology and the Swedish Research Council (VR), as well as the Swedish Foundation for Strategic Research (SSF) and the EU 7$^{\mathrm{th}}$ Framework Programme under GA n° ICT-619086 (MAMMOET).

References

[1] T. L. Marzetta, "Noncooperative cellular wireless with unlimited number of base station antennas," *IEEE Trans. Wireless Commun.*, vol. 9, pp. 3590–3600, Nov. 2010.

[2] F. Rusek, D. Persson, B. K. Lau, E. G. Larsson, T. L. Marzetta, O. Edfors, and F. Tufvesson, "Scaling up MIMO: Opportunities and challenges with very large arrays," *IEEE Signal Process. Mag.*, vol. 30, pp. 40–60, Jan. 2013.

[3] E. G. Larsson, F. Tufvesson, O. Edfors, and T. L. Marzetta, "Massive MIMO for next generation wireless systems," *IEEE Commun. Mag.*, vol. 52, pp. 186–195, Feb. 2014.

[4] H. Q. Ngo, E. G. Larsson, and T. L. Marzetta, "Energy and spectral efficiency of very large multiuser MIMO systems," *IEEE Trans. Wireless Commun.*, vol. 61, pp. 1436–1449, Apr. 2013.

[5] J. Andrews, S. Buzzi, C. Wan, S. Hanly, A. Lozano, A. Soong, and J. Zhang, "What will 5G be?," *IEEE J. Sel. Areas Commun.*, vol. 32, pp. 1065–1082, June 2014.

[6] F. Boccardi, R. Heath, A. Lozano, T. Marzetta, and P. Popovski, "Five disruptive techonology directions for 5G," *IEEE Commun. Mag.*, vol. 52, pp. 74–80, Feb. 2014.

[7] A. Osseiran, F. Boccardi, V. Braun, K. Kusume, P. Marsch, M. Maternia, O. Queseth, M. Schellmann, H. Schotten, H. Taoka, H. Tullberg, M. Uusitalo, B. Timus, and M. Fallgren, "Scenarios for 5G mobile and wireless communications: the vision of the METIS project," *IEEE Commun. Mag.*, vol. 52, pp. 26–35, May 2014.

[8] X. Gao, O. Edfors, F. Rusek, and F. Tufvesson, "Linear pre-coding performance in measured very-large MIMO channels," in *Proc. VTC 2011 Fall - IEEE 74th Vehicular Technology Conf.*, pp. 1–5, Sept. 2011.

[9] S. Payami and F. Tufvesson, "Channel measurements and analysis for very-large array systems at 2.6 GHz," in *Proc. EuCAP 2012 - 6th European Conf. in Ant. and Prop.*, pp. 433–437, Mar. 2012.

[10] X. Gao, F. Tufvesson, O. Edfors, and F. Rusek, "Measured propagation characteristics for very-large MIMO at 2.6 GHz," in *Proc. ASILOMAR 2013 - 46th Conf. on Sig., Syst. and Comput.*, pp. 295–299, Nov. 2012.

[11] X. Gao, O. Edfors, F. Rusek, and F. Tufvesson, "Massive MIMO in real propagation environments," *arXiv:1403.3376 [cs.IT], Submitted to IEEE Trans. Wireless Commun.*

[12] M. Costa, "Writing on dirty paper," *IEEE Trans. Inf. Theory*, vol. IT-29, pp. 439–441, May 1983.

[13] J. Hoydis, C. Hoek, T. Wild, and S. ten Brink, "Channel measurements for large antenna arrays," in *Proc. ISWCS 2012 - IEEE 9th Int. Symp. on Wireless Commun. Syst.*, vol. IT-29, pp. 811–815, Aug. 2012.

[14] R. S. Thomä, D. Hampicke, A. Richter, G. Sommerkorn, A. Schneider, U. Trautwein, and W. Wirnitzer, "Identification of time-variant directional mobile radio channels," *IEEE Trans. Instrum. Meas.*, vol. 49, pp. 357–364, Apr. 2000.

[15] S. Vishwanath, N. Jindal, and A. Goldsmith, "Duality, achievable rates, and sum-rate capacity of MIMO broadcast channels," *IEEE Trans. Inf. Theory*, vol. 49, pp. 2658–2668, Oct. 2003.

[16] N. Jindal, W. Rhee, S. Vishwanath, A. Jafar, and A. Goldsmith, "Sum power iterative water-filling for multi-antenna Gaussian broadcast channels," *IEEE Trans. Inf. Theory*, vol. 51, pp. 1570–1580, Apr. 2005.

[17] A. Paulraj, R. Nabar, and D. Gore, *Introduction to Space-Time Wireless Communications*. The Edinburg Building, Cambridge CB2 8RU, UK: Cambridge University Press, first ed., 2008.

[18] İ. E. Telatar, "Capacity of multi-antenna Gaussian channels," *Eur. Trans. Telecomm.*, vol. 10, no. 6, pp. 585–595, 1999.